RICHMOND
School of Arts & Sciences

Biology Faculty Publications   Biology

2-2016

Effects of a Pyrrole-Based, Microtubule-Depolymerizing Compound on RAW 264.7 Macrophages

John A. Ciemnieckia

Clarke P. Lewis

John T. Gupton
University of Richmond, jgupton@richmond.edu

Krista J. Stenger
University of Richmond, kstenger@richmond.edu

Follow this and additional works at: http://scholarship.richmond.edu/biology-faculty-publications

Part of the Biology Commons, and the Chemistry Commons

This is a pre-publication author manuscript of the final, published article.

Effects of a Pyrrole-Based, Microtubule-Depolymerizing Compound

on RAW 264.7 Macrophages

John A. Ciemniecki[a], Clarke P. Lewis[a], John T. Gupton[b], Krista Fischer-Stenger*[a]

[a]Department of Biology, University of Richmond, Richmond, VA 23173, United States

[b]Department of Chemistry, University of Richmond, Richmond, VA 23173, United States

Abstract

RAW 264.7 murine macrophages were exposed to the pyrrole-based compound 3,5-Dibromo-4-(3,4-dimethoxyphenyl)-1H-pyrrole-2-carboxylic acid ethyl ester (JG-03-14), which is a known microtubule depolymerizing agent with antitumor activity.[1,2,3,4] In this study exposure to JG-03-14 reduced the production of pro-inflammatory molecules by macrophages activated with lipopolysaccharide (LPS). Treatment with the pyrrole-based compound decreased the concentration of tumor necrosis factor-α (TNF-α) and nitric oxide (NO) released from the macrophages. Exposure to JG-03-14 also decreased TNF-α mRNA expression levels and the protein expression levels of inducible nitric oxide synthase (iNOS), the enzyme responsible for NO production in the activated macrophages. Furthermore, JG-03-14 treatment significantly changed the degradation profile of IκB-β, an inhibitor of the NF-κB transcription factor, which suggests that JG-03-14 may attenuate the activation of the LPS-induced NF-κB signaling

pathway needed to produce the pro-inflammatory mediators. We conclude that JG-03-14 possesses anti-inflammatory properties.

1. Introduction

Studies of 3,5-Dibromo-4-(3,4-dimethoxyphenyl)-1H-pyrrole-2-carboxylic acid ethyl ester (JG-03-14, Figure 1), a tetrasubstituted brominated pyrrole, have demonstrated that this compound possesses potent microtubule depolymerizing properties by binding tubulin at the colchicine site.[1,2,3] As a major component of the eukaryotic cytoskeleton, microtubules contribute to cell physiology by participating in chromosome segregation during mitosis, organelle trafficking and cell signaling events, and disruption of tubulin dynamics is the target of several anticancer drugs. Although colchicine was the first drug shown to bind tubulin, resulting in the loss of microtubules and the prevention of new microtubule formation, it is too toxic to be used in a clinical setting.[4,5,6] Therefore, less toxic compounds, such as JG-03-14, that bind at the colchicine site of tubulin have drawn considerable attention. Earlier studies that demonstrated the importance of the C-2 and C-4 positions of JG-03-14 for tubulin binding also showed that the tubulin-depolymerizing property of this compound correlated with anti-proliferative activity in a wide range of cancer cell lines.[2,3] Further investigations demonstrated that JG-03-14 promotes autophagic cell death of tumor cells and that it is active against tumor cells expressing the multidrug resistance pump, providing additional support for the potential use of JG-03-14 to treat

malignancies.[7,8] However, little is known about the effect of JG-03-14 on immune cells, specifically macrophages, which detect invading microorganisms in the tissues, carry out phagocytosis, and produce pro-inflammatory mediators.[9] While acute inflammation is protective against infections and tissue injury, chronic inflammation may lead to inflammatory disorders and cancers.[10,11,12,13,14] Studies have shown that other pyrrole-containing compounds possess anti-inflammatory properties.[15,16,17] Therefore, in addition to understanding the microtubule depolymerizing properties of JG-03-14, investigating the effects of JG-03-14 on the pro-inflammatory activity of macrophages is important in order to expand our knowledge of the compound's bioactive properties and its clinical potential.
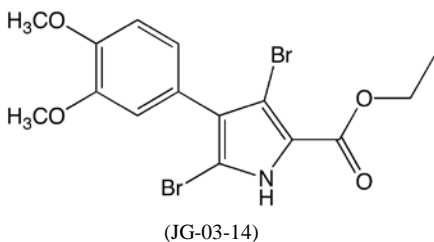

(JG-03-14)

Figure 1. Structure of 3,5-Dibromo-4-(3,4-dimethoxyphenyl)-1H-pyrrole-2-carboxylic acid ethyl ester (JG-03-14).

The Nuclear Factor-kappa B (NF-κB) transcription factor is one of the most important regulators of the inflammatory response. In macrophages, the pro-inflammatory NF-κB signaling pathway can be activated by lipopolysaccharide (LPS), a cell wall component of gram-negative bacteria, which binds to the Toll-like receptor 4 (TLR4) complex and triggers the production of pro-inflammatory molecules.[9] Initiation of this pathway involves a complex signaling architecture that ultimately phosphorylates and activates the IKK complex, which in turn phosphorylates the inhibitory proteins IκB-α and IκB-β that are bound to the NF-κB transcription factor.[18] These inhibitory proteins are then ubiquitinated and degraded in a cytosolic proteasome.[18] The now-active NF-κB translocates into the nucleus and promotes the

transcription of inflammatory response genes. In mice, some of these genes include *TNFA,* which encodes the cytokine tumor necrosis factor-α (TNF-α) and *NOS2*, which encodes inducible nitric oxide synthase (iNOS). The iNOS enzyme catalyzes the reaction of L-arginine to citrulline, which produces nitric oxide (NO) radicals as a byproduct, useful as both a vasodilator and an anti-pathogenic oxidant.

To assess the effects of JG-03-14 on the macrophage inflammatory response, our study investigated how exposure to JG-03-14 affected the production of NO, iNOS, and TNF-α by RAW 264.7 macrophages activated with LPS. We also investigated JG-03-14's effects on the relative mRNA expression of TNF-α as well as the degradation of the IκB-β inhibitory protein after LPS activation. We found that JG-03-14 suppressed the production of the inflammatory molecules and our data further suggest that this may be caused by an effect on the NF-κB signaling pathway.

2. Materials and methods

2.1 Cell Culture

RAW 264.7 macrophages were purchased from ATCC and plated in T75 filter-top flasks, where they were managed under sterile conditions and grown at 37°C with 5% CO_2. Cells were maintained in RPMI complete medium containing 10% fetal calf serum and supplemented with L-glutamine, non-essential amino acids, MEM vitamins, and penicillin/streptomycin and grown to approximately 75-95% confluence. Cell populations were activated with LPS (E. coli 055:B5; Sigma-Aldrich). Cell lysates and supernatants were harvested 2.5 minutes to 2 hours after LPS-activation for IκB-β experiments, 4 hours after activation for TNF-α experiments, and 20 hours after activation for NO/iNOS studies. The JG-03-14 compound was provided by Dr. John

4

Gupton and solubilized in DMSO, and then diluted in fresh medium (to < 1% DMSO) before being added to culture media. In all experiments, JG-03-14 compound was administered 1 hour before LPS activation. After LPS incubation, cell culture supernatants were collected. Adherent cells were then washed twice with phosphate buffered saline (PBS), and homogenized with lysis buffer consisting of 0.05 M Tris buffer (pH 7.5), 0.3 M NaCl, 2 mM EDTA, 0.5% Triton-X 100, 2 µg/mL Leupeptin (Sigma-Aldrich), 1 µg/mL Aprotinin (Sigma-Aldrich), and 0.2 mM PMSF (Sigma-Aldrich). Both supernatants and lysates were stored at -20°C until assayed.

2.2 Fluorescence Microscopy

Cells were plated on coverslips held in 6-well plates and allowed to adhere overnight. After exposure to JG-03-14 and a 4-hour LPS activation period, cells were washed with PBS, fixed with paraformaldehyde for 10 minutes, washed with 0.5% Triton-X in PBS for 5 minutes, and then placed in a donkey serum blocking solution for 30 minutes. Cells were then incubated in 1 ug/mL mouse anti-α-tubulin antibody by placing coverslips facedown on a parafilm surface in the antibody diluted in the block solution for 30 minutes. The coverslips were then washed in PBS for 5 minutes four times. Cells were then incubated in 1:4000 dilution of DAPI, 1:1000 dilution of phalloidin, and 1:10,000 dilution of donkey anti-mouse antibody conjugated to ALEXA 488 for 30 minutes. The coverslips were again washed in PBS for 5 minutes four times. Coverslips were then mounted onto microscope slides in glycerol mounting media and sealed with clear nail polish. Images were acquired using an Olympus IX-83 microscope outfitted with a PLAN APON 60x/1.42NA DIC objective, an EXFO mixed gas light source, Sutter filter wheels and shutters, a Hamamatsu ORCA-Flash 4.0 V2 sCMOS camera, and Metamorph imaging software. Z-stack images (0.2 µm steps) were captured sequentially using the Sedat

Quad filter-set (Chroma), and exposure times were maintained constant within an experimental data set.

2.3 MTT Cell Viability Assay

MTT compound (Sigma-Aldrich) was solubilized in PBS in limited light conditions at a concentration of 5 mg/mL and left overnight at 4°C to dissolve completely. Populations of 5.0 x 10^3 cells were added to wells in a 96-well flat-bottom microtiter plate and were allowed to adhere for 2 hours before media was aspirated and replaced with 100 mL fresh media. Cells were then administered JG-03-14 and underwent a 20-hour incubation. Next 10 uL of the MTT solution were added to each well in limited light conditions and allowed to incubate in the dark for 4 hours in the CO_2 incubator. The formazan crystals were solubilized with 100 uL of isopropanol in 0.04 M HCl. Absorbance was immediately read at 570 nm using a Beckman-Coulter DTX 800 Multimode Detector. It is also important to note that for all experiments performed in this study microscopic examination did not detect any noticeable differences in the viability of cultures, regardless of treatment (data not shown).

2.4 Nitric Oxide Assay

Populations of 3.3 x 10^6 cells were incubated with LPS for 20 hours before being harvested for NO assessment. Nitrite accumulation in the supernatants was assessed using a standard Greiss assay. Briefly, an equal volume of supernatant (50 μL) was reacted with equal volumes of each Greiss reagent (50 μL each) and the absorbance was read at 550 nm using a Beckman-Coulter DTX 800 Multimode Detector.

2.5 Western Blotting

Populations of 3.3 x 10^6 (for iNOS) and 5.0 x 10^5 cells (for IκB-β) were treated as previously described. Thirty μg of protein from each cell lysate was separated on a 10% gel (Bio-Rad Mini-PROTEAN TGX Stain-Free Pre-Cast Gels) and transferred to a nitrocellulose membrane (Bio-Rad). Membranes were blocked for 1 hour with 5% non-fat dry milk solubilized in Tris-buffered saline (TBS), followed by a 5 minute TBS wash. To detect the protein of interest, the membranes were incubated overnight at 4°C with the primary antibody (Santa-Cruz Biotechnologies) diluted 1:200 in TBST (TBS with 0.2% non-fat dry milk and 0.1% Tween-20). The membrane was then washed three times for 10 minutes in TBST and incubated with the appropriate secondary antibody (Santa-Cruz Biotechnologies) diluted 1:7500 in TBST for 1 hour at room temperature with gentle agitation. The membrane was then washed four times for 5 minutes each in TBST and visualized using GE Healthcare Amersham ECL Western Blotting detection reagents and Kodak Biomax XAR Film. Blots were stripped with Millipore Re-Blot Plus Mild Antibody Stripping Solution according to the manufacturer's instructions and re-probed using a mouse anti-actin antibody (Sigma-Aldrich) at a 1:5000 dilution using the previously described procedure.

2.6 TNF-α ELISA

Populations of 3.3 x 10^6 cells were treated as previously described. Supernatant samples collected from the cultures were diluted 1:100 then analyzed to quantify the presence of TNF-α using an OptEIA^{TM} ELISA assay (BD Biosciences). Protocol was carried out according to the manufacturer's directions.

2.7 TNF-α qPCR

Populations of 3 x 10^5 cells were treated as previously described. RNA from these cultures was harvested using the Qiagen RNEasy Mini-Kit. After RNA was collected, cDNA was created using Origene's First-Strand cDNA Synthesis Kit following Origene's standard protocols and using a Bio-Rad DNAEngine thermo-cycler. The gene of interest was amplified using Origene primers (qSTAR qPCR primer pairs against *Mus musculus* Tnf and Actb) and Quanta Biosciences B-R SYBR Green SuperMix for iQ in 20 μL reactions. Reaction progress was monitored using a Bio-Rad CFX Connect Real-Time System and its associated software. C_q data were analyzed using a normalized expression method ($\Delta\Delta C_q$).

2.8 IκB-β Densitometry and Analysis

Densitometry of IκB-β western blots was completed using a Kodak Gel Logic 200 imaging system and its associated software. Densities were normalized against the initial density of IκB-β on each blot. The relative density values were then linearized assuming exponential decay by taking the natural logarithm of the relative densities. The best-fit linear slope was then averaged between independent experimental replicates for comparison. Standard error was calculated from the variability of this slope between replicates but not the variability from the fit of the individual data sets to a linear trend. The minimum relative densities were also averaged between independent experimental replicates for comparison, and once again standard error was calculated from the variability of these relative density minima.

2.9 Statistics

All data were analyzed using Graphpad PRISM software and a one-way ANOVA test, except for IκB-β densitometry data, which utilized heteroscedastic two-tailed t-tests for comparison of the means.

3. Results

3.1 Microtubule network

The microtubule-depolymerizing effects of JG-03-14 were confirmed using fluorescence microscopy of RAW 264.7 cells treated with JG-03-14 with and without subsequent LPS activation (Figure 2). Qualitative assessment showed that resident macrophages demonstrated consistent, diffuse distribution of microtubules, while activation of these macrophages with LPS increased microtubule organizing center (MTOC) brightness and microtubule network complexity. This is consistent with previous studies.[19,20] When pretreated with JG-03-14, the cells failed to construct a diffuse microtubule network as seen in the resident macrophages, however, LPS activation still increased MTOC brightness despite the lack of a clear microtubule network.
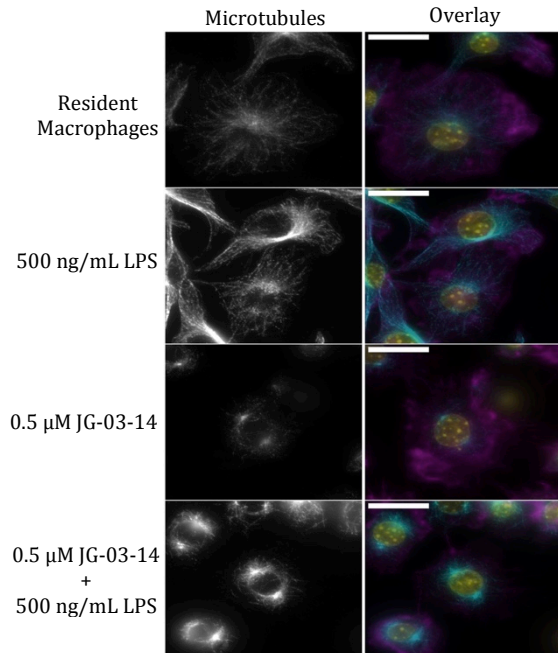
Figure 2. Effect of JG-03-14 on microtubule polymerization and distribution in RAW 264.7 cells. Cells were treated with JG-03-14 one hour before a 4 hour LPS activation, fixed with paraformaldehyde, and stained with anti-α-tubulin antibody (Alexa 488), DAPI, and Phalloidin (Alexa 568). Images are shown on the same brightness scale as a z-stack composite and were taken with the same exposure time. Overlay shows f-actin (Phalloidin) in magenta, microtubules (Alexa 488) in cyan, and nuclei (DAPI) in yellow. White scale bar is 20 μm.

3.2 Cell viability

Next, RAW 264.7 cells in culture were assessed for viability across a range of JG-03-14 concentrations over a 21-hour incubation period. A slight decrease in cell viability was detected after exposure to concentrations up to eight times those used in this study (Figure 3).
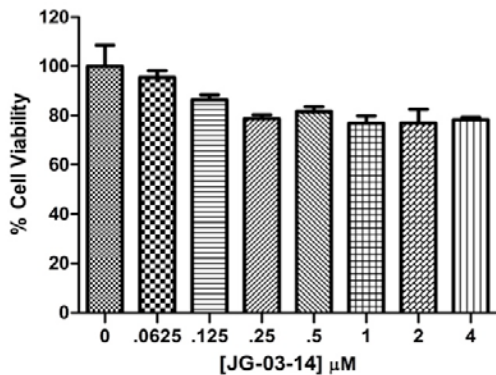
Figure 3. Effect of JG-03-14 on RAW 264.7 Cell Viability. Populations of 5,000 cells were exposed to varying concentrations of JG-03-14 for 20 hours. Viability was assessed using an MTT assay and is reported as a percentage of the control sample. Representative figure of an experiment conducted in independent triplicate.

3.3 Production of pro-inflammatory molecules

In order to assess the effects of JG-03-14 on the inflammatory response, we analyzed NO production by LPS-activated RAW 264.7 cells with and without JG-03-14 pretreatment using a standard Greiss assay. We found that NO production was significantly reduced in cells pretreated for one hour with 0.5 μM JG-03-14 and activated with 500 ng/mL LPS (Figure 4a). Corresponding iNOS levels within the lysates from the same cells were also examined using western blot analysis, and results correlated with NO levels (Figure 4b). We also measured TNF-α released from the macrophages using an ELISA and found the amount of secreted TNF-α to be significantly reduced in cells pretreated with either 0.25 or 0.5 μM JG-03-14 (Figure 5a). We then used qPCR to compare the relative *TNFA* expression levels between activated macrophages exposed to JG-03-14 and those that were not. Relative expression levels of *TNFA* mRNA were found to be decreased in cultures pretreated with either 0.25 or 0.5 μM JG-03-14 (Figure 5b).
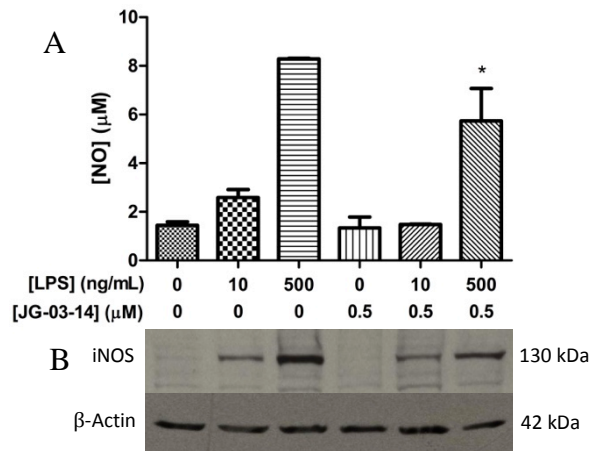
Figure 4. Effect of JG-03-14 on NO and iNOS production in activated RAW 264.7 macrophages. Cells were pretreated with JG-03-14 one hour before LPS activation. Cells were incubated 20 hours after LPS activation. (A) Nitric oxide production in activated RAW 264.7 macrophages. (B) Western blot showing iNOS production in the same sample of RAW 264.7 macrophages. Both are representative of an experiment conducted in independent triplicate. *$p < 0.05$.
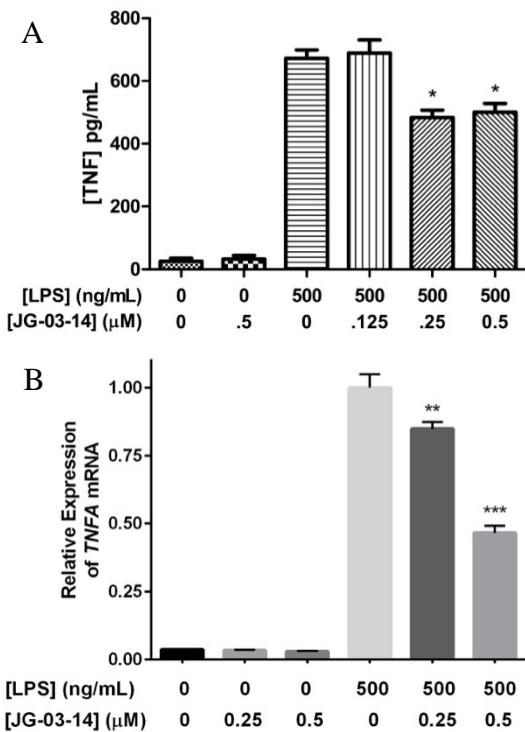

Figure 5. Effect of JG-03-14 on TNF-α and TNFA mRNA production in activated RAW 264.7 macrophages. Cells were pretreated with JG-03-14 1 hour before LPS activation, then incubated 4 hours. (A) Concentration of TNF-α secreted protein as measured by ELISA (B) Relative expression of TNFA mRNA as measured by qPCR. Representative figures of experiments conducted in independent triplicate. Means compared to LPS control using one-way ANOVA. *$p < 0.05$, **$p < 0.01$, ***$p < 0.001$.

3.4 NF-κB activation

We hypothesized that the attenuation of iNOS and TNF-α protein expression may be due to an effect that JG-03-14 has on the activation of the NF-κB transcription factor. To assess the effect of the compound on the NF-κB activation in RAW 264.7 macrophages, we tracked the relative amounts of IκB-β over time within the macrophages using western blot analysis. Our results show that pretreatment with JG-03-14 significantly altered the degradation profile of IκB-β within activated RAW 264.7 macrophages (Figure 6a and 6b). Densitometry of the bands representing IκB-β protein relative to the band at $t = 0$ was used to quantify and analyze the effect of JG-03-14 on the degradation of IκB-β (Figure 6c). In order to assess differences in the IκB-β degradation rate between the cells pretreated with 0.5 μM JG-03-14 and those that were not, the densitometry data were linearized assuming exponential decay and a best-fit linear slope was found for each of the resultant data. The magnitude of the slope was found to be significantly decreased when analyzed from cells pretreated with 0.5 μM JG-03-14 (figure 7a), indicating that the rate of decay of the steady state amount of IκB-β within the cells after LPS activation was also decreased. Furthermore, the minimum density band on each blot was found and averaged between independent experiments. The minimum IκB-β level in the activated cells during the first two hours after LPS activation was found to be increased by about 20% in cells pretreated for one hour with 0.5 μM JG-03-14 (Figure 7b), indicating that the minimum steady-state amount of IκB-β in the cells was significantly greater in the cells pretreated with JG-03-14. These results, taken together with the observed decrease in production of inflammatory molecules by activated macrophages, suggest that exposure to JG-03-14 may be suppressing NF-κB's ability to promote pro-inflammatory gene transcription in response to LPS stimulation.
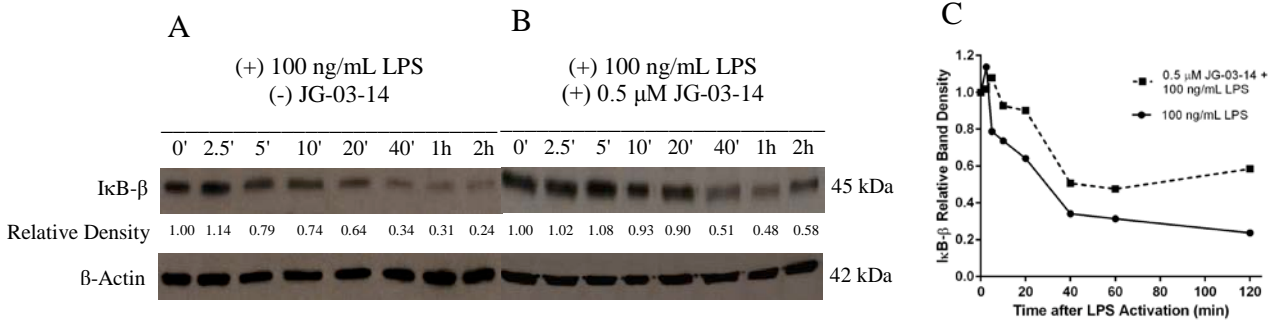
13

Figure 6. Effect of JG-03-14 on steady-state amount of IκB-β over time. (A) Cells were activated with LPS and lysed at indicated time points and analyzed by western blotting. (B) Cells were treated with JG-03-14 for 1 hour, then activated with LPS and lysed at indicated time points. (C) Relative densitometry representation of (A) and (B). Band densities normalized to the initial IκB-β band (0' time point) on the respective blot. Representative figures of experiments conducted in independent triplicate.
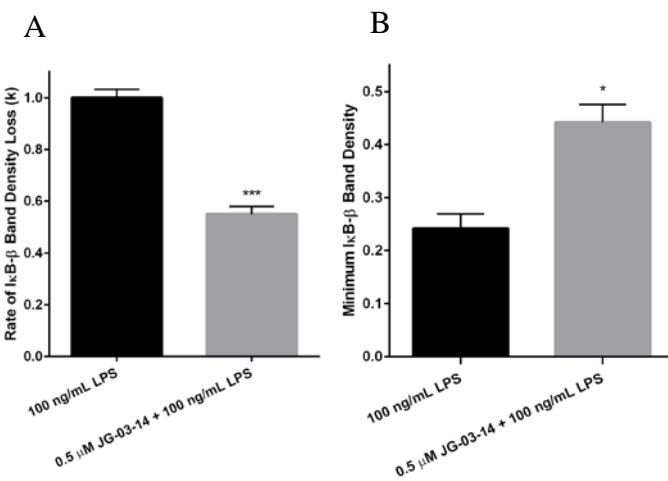

Figure 7. Analysis of IκB-β densitometry. (A) Densitometry data were linearized assuming an exponential decay trend ($D = e^{-kt}$, where D is the relative densitometry value, t is the time in minutes, and k is the rate of decay), and the best-fit linear slopes for each treatment were compared. (B) Minimum IκB-β band densities relative to the $t = 0$ band density in the corresponding data set for each treatment were compared. In each comparison, means were calculated from data collected from three independent experiments, and compared using a heteroscedastic two-tailed t-test. **p<0.01, ***p<0.001.

4. Discussion

Previous studies have shown that JG-03-14 possesses potent microtubule depolymerizing and anti-tumor activity, lending support to the compound's potential as a cancer chemotherapeutic

agent.[1,7,8] We have shown that JG-03-14 disrupts microtubule polymerization and distribution within RAW 264.7 cells, and in activated macrophages it decreases the production of iNOS and NO radicals as well as TNF-α mRNA and protein. JG-03-14 also delays and decreases the degradation of the IκB-β protein, one of the inhibitory proteins whose degradation is coupled with the activation of the NF-κB transcription factor that is responsible for the induction of pro-inflammatory genes. Our data, therefore, indicate that JG-03-14 also possesses anti-inflammatory properties, adding support to other studies demonstrating the anti-inflammatory properties of pyrrole compounds.[15,16,17]

The change in the IκB-β degradation profile due to pretreatment with JG-03-14 could have multiple independent or inter-related causes. The study we conducted showed the change in the steady-state amount of IκB-β over time after macrophage activation, which can be affected both by the kinetics of IκB-β degradation and resynthesis of the protein. It is also known that newly synthesized IκB-β in a hypophosphorylated form can bind to NF-κB in the nucleus without inhibiting NF-κB's ability to bind to DNA and promote gene transcription.[21] Our technique did not discriminate between IκB-β with and without post-translational modifications. Therefore, there are several ways that JG-03-14 may be mediating the observed anti-inflammatory effect. While it is possible that the destabilization of microtubules by JG-03-14 could be disrupting vesicle trafficking resulting in a reduction in TNF-α secreted by the macrophages, our results also suggest that this compound may directly affect the components of the LPS-induced NF-κB pathway, or possibly alter the events leading to the degradation of IκB-β. Another intriguing possibility is that JG-03-14's effect on NF-κB activation is a consequence of its anti-microtubule activity, which would suggest a connection between the microtubule network and the LPS-induced NF-κB pathway. Recent studies showing a connection between

cytoskeletal proteins and the activation and/or kinetics of the NF-κB pathway make this possibility an important foundation for future inquiry.[22] Furthermore, a study published in 1992 reported that the compound taxol, a potent microtubule stabilizer, exerted LPS-like effects upon macrophages by inducing the mRNA expression of TNF-α and interleukin-1β in the absence of LPS.[23] The fact that a microtubule stabilizer induced the expression of pro-inflammatory products in that study and a microtubule destabilizer repressed pro-inflammatory products in the present one may be a coincidence, but it warrants further investigation. These future studies may reveal a novel interaction between microtubules and the signaling components responsible for the activation of NF-κB.

If JG-03-14 is instead found to have a direct interaction with the signaling components of the NF-κB pathway, it may increase its potential as an anti-tumor agent. Indeed, many cancers are exacerbated by a constitutively active NF-κB transcription factor, which can be caused by various perturbations or mutations in the normal pathway and its signaling termination programs.[13,24] A compound that has anti-tumor properties while also debasing a cancer cell's resistance to chemotherapeutics may have clinical attractiveness for treating more aggressive cancers. Besides elucidating the targets of JG-03-14, it would also be prudent to test JG-03-14's anti-tumor efficacy on aggressive cancer types known to contain aberrations in their NF-κB signaling machinery.

Author information

Corresponding Author

*Krista Fischer-Stenger: Department of Biology, 28 Westhampton Way, Gottwald Science

Center, University of Richmond, VA 23173, Tel: (804) 287-6570, Fax: (804) 289-8233, Email:

kstenger@richmond.edu

Present Addresses

[a]John Ciemniecki, Department of Biology, 28 Westhampton Way, Gottwald Science Center,

University of Richmond, VA 23173, Email: john.ciemniecki@richmond.edu

[a]Clarke Lewis, Department of Biology, 28 Westhampton Way, Gottwald Science Center,

University of Richmond, VA 23173, Email: clarke.lewis@richmond.edu

[b]John Gupton, Department of Chemistry, 28 Westhampton Way, Gottwald Science Center,

University of Richmond, VA 23173, Email: jgupton@richmond.edu

[a]Krista Stenger, Department of Biology, 28 Westhampton Way, Gottwald Science Center,

University of Richmond, VA 23173, Email: kstenger@richmond.edu

Author Contributions

This manuscript was written through contributions of all authors. JC and KFS drafted the

manuscript. JG synthesized and provided JG-03-14 for the studies. JC performed the

fluorescence microscopy. JC and CL performed the western blots, ELISAs, nitric oxide assays,

and cell viability assays. JC conducted the IκB-β experiments. KFS, JC, and CL analyzed all

data. All authors read, edited and approved the final manuscript.

Funding Sources

Acknowledgment

Abbreviations

NF-κB, Nuclear factor kappa B; LPS, Lipopolysaccharide; TLR4, Toll-like receptor 4; IKK, Inhibitor of nuclear factor kappa B kinase; IκB-α, Inhibitor of nuclear factor kappa B alpha; IκB-β, Inhibitor of nuclear factor kappa B beta; TNF-α, Tumor necrosis factor alpha; iNOS, Inducible nitric oxide synthase; NO, Nitric oxide; MTOC, Microtubule organizing center.

References

[1] Mooberry, S. L.; Weiderhold, K. N.; Dakshanamurthy, S.; Hamel, E.; Banner, E. J.; Kharlamova, A.; Hempel, J.; Gupton, J. T.; Brown, M. L. Identification and characterization of a new tubulin-binding tetrasubstituted brominated pyrrole. *Mol. Pharmacol.* **2007**, *72*, 132-140.

[2] Da, C.; Telang, N.; Barelli, P.; Jia, X.; Gupton, J. T.; Mooberry, S. L.; Kellogg, G. E. Pyrrole-Based Antitubulin Agents: Two Distinct Binding Modalities are Predicted for C-2 Analogues in the Colchicine Site. *Med. Chem. Lett.* **2012**, 3, 53-57.

[3] Da, C.; Telang, N.; Hall, K.; Kluball, E.; Barelli, P.; Finzel, K.; Jia, X.; Gupton, J. T.; Mooberry, S. L.; Kellogg, G. E. Developing novel C-4 analogues of pyrrole-based antitubulin agents: weak but critical hydrogen bonding in the colchicine site. *Med. Chem. Commun.* **2013**, 4, 417-421.

[4] Owellen, R. J.; Owens, A. H., Jr.; Donigian, D. W. The binding of vincristine, vinblastine and colchicine to tubulin. *Biochem. Biophys. Res. Comm.* **1972**, 47, 685-691.

[5]Jordan, A.; Hadfield, J. A.; Lawrence, N. J.; McGown, A. T. Tubulin as a target for anticancer drugs: agents which interact with mitotic spindle. *Med. Res. Rev.* **1998**, 18, 259-296.

[6]Stanton, R. A.; Gernert, K. M.; Nettles, J. H.; Aneja, R. Drugs that target dynamic microtubules: a new molecular perspective. *Med. Res. Rev.* **2011**, 31, 443-481.

[7]Arthur, C. R.; Gupton, J. T.; Kellogg, G. E.; Yeudall, W. A.; Cabot, M. C.; Newsham, I.; Gewirtz, D. A. Autophagic cell death, polyploidy and senescence induced in breast tumor cells by the substituted pyrrole JG-03-14, a novel microtubule poison. *Biochem. Pharm.* **2007**. 74, 981-991.

[8]Biggers, J. W.; Nguyen, T.; Di, X.; Gupton, J. T.; Henderson, S. C.; Emery, S. M.; Moureq, A.; White, K. L.; Brown, R.; Almenara, J.; Gewirtz, D. A. Autophagy, cell death and sustained senescence arrest in B16/F10 melanoma cells and HCT-116 colon carcinoma cells in response to the novel microtubule poison, JG-03-14. *Cancer Chemother. Pharmacol.* **2013**, *71*, 441-455.

[9]Gordon, S. Pattern recognition receptors: doubling up for the innate immune response. *Cell.* **2002**. 111, 927-930.

[10]Chai, E. Z. P.; Siveen, K. S.; Shanmugam, M. K.; Arfuso, F.; Sethi, G. Analysis of the intricate relationship between chronic inflammation and cancer. *Biochem. J.* **2015**, 468, 1-15.

[11]He, Y.; Yue, Y.; Zheng, X.; Zhang, K.; Chen, S.; Du, Z. Curcumin, inflammation, and chronic diseases: How are they linked? *Molecules.* **2015**, 20, 9183-9213.

[12]Schuliga, M.; NF-kappaB signaling in chronic inflammatory airway disease. *Biomolecules.* **2015**, 5, 1266-1283.

[13]Verstrepen, L.; Beyaert, R.; Receptor proximal kinases in NF-κB signaling as potential therapeutic targets in cancer and inflammation. *Biochem. Pharmacol.* **2014**, 92, 519-529.

[14]Woo, J. H.; Lee, J. H.; Kim, H.; Park, S. J.; Joe, E.; Jou, I. Control of inflammatory responses: a new paradigm for the treatment of chronic neuronal diseases. *Exp. Neurobiol.* **2015**, 2, 95-102.

[15]Mohamed, M.S.; Kamel, R.; Fathallah, S. S. Synthesis of New Pyrroles of Potential Anti-Inflammatory Activity. *Arch. Pharm. Chem. Life Sci.* **2011**. *344*, 830-39.

[16]Maddila, S.; Gorle, S.; Sampath, Ch.; Lavanya, P. Synthesis and anti-inflammatory activity of some new 1,3,4-thiadiazoles containing pyrazole and pyrrole nucleus. *Journal of Saudi Chem. Soc.* **2012**.

[17]Battilocchio, C.; Poce, G.; Alfonso, S.; Porretta, G. C.; Consalvi, S.; Sautebin, L.; Pace, S.; Rossi, A.; Ghelardini, C.; Di Cesare Mannelli, L.; Schenone, S.; Giordani, A.; Di Francesco, L.; Patrignani, P.; Biava, M. A class of pyrrole derivatives endowed with analgesic/anti-inflammatory activity. *Bioorganic and Med. Chem.* **2013**. *21*, 3695-701.

[18]Hayden, M.; Ghosh, S. NF-κB, the first quarter-century: remarkable progress and outstanding questions. *Genes & Dev.* **2012**. *26*, 203-234.

[19]Robinson, J.; Vandré, D. Stimulus-dependent alterations in macrophage microtubules: increased tubulin polymerization and detyrosination. *Cell Sci.* **1995**. *108*, 645-55.

[20]Patel, P.; Fisher, K.; Yang, E.; Deane, C.; Harrison, R. Proteomic analysis of microtubule-associated proteins during macrophage activation. *Mol. and Cell. Proteomics.* **2009**. *8.11*, 2500-14.

[21]Suyang, H.; Phillips, R.; Douglas, I.; Ghosh, S. Role of Unphosphorylated, Newly Synthesized IκBβ in the Persistent Activation of NF-κB. *Mol. and Cell. Bio.* **1996**. *16*, 5444-9.

[22]Davuluri, G.; Augoff, K.; Schiemann, W.; Plow, E.; Sossey-Alaoui, K. WAVE3-NFκB Interplay is Essential for the Survival and Invasion of Cancer Cells. *PLOS ONE.* **2014**. *9.10*, 1-13.

[23]Bogdan, C.; Ding, A. Taxol, a microtubule-stabalizing antineoplastic agent, induces expression of tumor necrosis factor α and interleukin-1 in macrophages. *Leuk. Biol.* **1992**, *52*, 119-121.

[24]Dolcet, X.; Llobet, D.; Pallares, J.; Matias-Guiu; X. NF-κB in development and progression of human cancer. *Virchows Arch.* **2005**. *446*, 475-482.